THE JOURNAL OF BIOLOGICAL CHEMISTRY
Vol. 279, No. 6, Issue of February 6, pp. 4829–4839, 2004
Printed in U.S.A.

Centrosomal Anchoring of Protein Kinase C βII by Pericentrin Controls Microtubule Organization, Spindle Function, and Cytokinesis*

Received for publication, October 11, 2003, and in revised form, October 22, 2003
Published, JBC Papers in Press, November 1, 2003, DOI 10.1074/jbc.M311196200

Dan Chen‡§¶, Aruna Purohit¶‖, Ensar Halilovic‖, Stephen J. Doxsey‖, and Alexandra C. Newton‡ ‡‡**

From the ‡Department of Pharmacology, §Molecular Pathology Graduate Program, School of Medicine, University of California at San Diego, La Jolla, California 92093-0640 and the ‖Department of Molecular Medicine, University of Massachusetts Medical School, Worcester, Massachusetts 01605

Location is a critical determinant in dictating the cellular function of protein kinase C (PKC). Scaffold proteins contribute to localization by poising PKC at specific intracellular sites. Using a yeast two-hybrid screen, we identified the centrosomal protein pericentrin as a scaffold that tethers PKC βII to centrosomes. Co-immunoprecipitation studies reveal that the native proteins interact in cells. Co-overexpression studies show that the interaction is mediated by the C1A domain of PKC and a segment of pericentrin within residues 494–593. Immunofluorescence analysis reveals that endogenous PKC βII colocalizes with pericentrin at centrosomes. Disruption of this interaction by expression of the interacting region of pericentrin results in release of PKC from the centrosome, microtubule disorganization, and cytokinesis failure. Overexpression of this disrupting fragment has no effect in cells lacking PKC βII, indicating a specific regulatory role of this isozyme in centrosome function. These results reveal a novel role for PKC βII in cytokinesis and indicate that this function is mediated by an interaction with pericentrin at centrosomes.

Protein kinase C (PKC)[1] family members transduce an abundance of signals that mediate lipid hydrolysis. Their function is exquisitely regulated by subcellular location, mediated by both lipid and protein interactions (1–4). One key emerging function of PKC family members is the regulation of cell growth, cell cycle progression, and cell differentiation (5, 6). Studies have shown that PKC α and PKC δ play an important role in negative regulation of the G_1/S and G_2/M transition (7, 8). PKC βII has been shown to be critical for nuclear lamina disassembly at the G_2/M transition through phosphorylation of lamin B in K562 erythroleukemia cells (9). An essential role in cell cycling is illustrated in yeast, where there is only one PKC, and deletion of this gene traps cells in a G_2-like arrest following completion of DNA synthesis (10). However, the role of anchoring PKC to subcellular sites in the control of cell cycle progression is largely unexplored.

Centrosomes are small organelles in vertebrate cells that serve primarily as organizers of microtubules. A number of converging studies suggest that centrosomes are involved in an increasing number of fundamental cellular processes including cell cycle progression, microtubule organization, spindle function, and cytokinesis (11). Treatment of cells with phorbol esters, potent activators of PKC, has been long known to cause dramatic morphological changes (12). Many of these changes result from alterations in cytoskeletal structure, and several lines of evidence implicate PKC in regulating microtubule function. First, a number of microtubule-associated proteins are substrates for PKC both *in vitro* and *in vivo* (13, 14); second, phorbol esters cause microtubule reorganization (15, 16); third, PKC βI has been shown to co-localize with microtubules and bind microtubule-associated proteins (15); and fourth, novel PKC isoforms ϵ and δ have been reported to localize to the centrosome (17, 18). Importantly, recent studies demonstrate that PKC β-deficient T cells failed to develop a polarized microtubule network, a defect that can be rescued by expressing PKC βI (19). Thus, PKC is emerging as a key regulator of microtubule organization. However, the molecular mechanism has remained elusive.

Pericentrin is a coiled-coil protein that is thought to mediate microtubule anchoring at the centrosome by binding a multiprotein complex that nucleates microtubules, the γ-tubulin ring complex (20, 21). Pericentrin belongs to a family of related proteins, including CG-NAP/AKAP450 and kendrin (22–25). Functional studies have revealed a key role for pericentrin in microtubule organization, spindle assembly, and chromosome segregation (20). Overexpression of pericentrin causes microtubule defects, chromosome missegregation, and aneuploidy (26).

In this study, we identified pericentrin as a binding partner for PKC from a yeast two-hybrid screen. Co-immunoprecipitation studies reveal that the endogenous proteins interact in cells, and biochemical studies narrow the interaction domains to the C1A domain in PKC and residues 494–593 in pericentrin. We show that disruption of the pericentrin-PKC interaction by overexpressing the binding domain on pericentrin (residues 494–593) results in the mislocalization of PKC βII from the centrosome, microtubule disorganization, cytokinesis failure, spindle dysfunction, chromosome missegregation, and aneuploidy. These data suggest a novel role for PKC in controlling cell division through centrosomal anchoring by pericentrin.

EXPERIMENTAL PROCEDURES

Materials—The large T-antigen-transformed human embryonic kidney cells (tsA201) were the generous gift of Dr. Marlene Hosey (North-

* This work was supported by National Institutes of Health Grants P01 DK54441 (to A. C. N.) and GM51994 (to S. J. D.). The costs of publication of this article were defrayed in part by the payment of page charges. This article must therefore be hereby marked "*advertisement*" in accordance with 18 U.S.C. Section 1734 solely to indicate this fact.

¶ These authors contributed equally to this work.
** To whom correspondence may be addressed. Tel.: 508-856-1613; Fax: 508-856-4289; E-mail: Stephen.Doxsey@umass.med.edu.
‡‡ To whom correspondence may be addressed. Tel.: 858-534-4527; Fax: 858-534-6020; E-mail: anewton@ucsd.edu.

[1] The abbreviations used are: PKC, protein kinase C; HA, hemagglutinin; GFP, green fluorescent protein; GST, glutathione *S*-transferase.

western University). The rat intestinal epithelial cells (RIE-1) were the gift of Dr. Alan Fields (Mayo Clinic). The cDNA of rat PKC βII was a gift of Dr. Daniel E. Koshland, Jr. (University of California, Berkeley), and the cDNA of wild-type and kinase-dead PKC α, ϵ, and ζ were gifts of Dr. Alex Toker (Harvard Medical School). A polyclonal antibody against PKC βII (C-18, α-PKC βII) and protein A/G-agarose were purchased from Santa Cruz Biotechnology, Inc. (Santa Cruz, CA). A monoclonal antibody against a determinant in the regulatory domain of PKC β (α-Reg) was purchased from Transduction Laboratories. A monoclonal antibody 16B12 against the hemagglutinin (HA) epitope and a monoclonal antibody against the GFP epitope were purchased from Covance. PKC βII was purified from the baculovirus expression system, as previously described (27). A polyclonal antibody, UM225, was made against the N-terminal peptide sequence of pericentrin (EAQEQHARELQL). Antibodies to α- and γ-tubulin were obtained from Sigma. Anti-HA polyclonal antibody was a gift from Joanne Buxton (University of Massachusetts Medical School). 5051 human autoimmune serum, and anti-pericentrin polyclonal antibody were used in this study (20). A polyclonal antibody against the GFP epitope was a gift from Pam Silver (Dana-Farber Cancer Institute). Mouse anti-dynein cytoplasmic monoclonal antibody was purchased from Chemicon international Co.

Yeast Two-hybrid Screen—The cDNA encoding rat PKC βII (residues 1–111) was amplified by PCR and inserted into the NcoI site (5′ site) and the BamHI site (3′ site) of pAS2.1 (Clontech). The resulting plasmid was used as bait to screen a cDNA library derived from 9.5- and 10.5-day mouse embryos (28). Approximately 100,000 yeast CG1945 transformants were grown in the absence of tryptophan, leucine, and histidine at 30 °C for 8 days. Colonies that grew in this minimal selective medium condition were scored for β-galactosidase activity by colony lift assay according to the Clontech MatchMaker protocol. Prey plasmid DNA from the double-positive ($His^+/LacZ^+$) colonies was rescued by electroporation into *Escherichia coli* HB101 (Invitrogen) and then retransformed back into yeast strain SFY526 containing the original bait plasmid and various control plasmids for one-to-one interactions. Both strands of the DNA insert from these clones were sequenced by automated sequencing (DNA Sequencing Shared Resource, Cancer Center, University of California, San Diego).

Plasmid Constructs—Mammalian expression constructs encoding the N-terminally HA-tagged full-length pericentrin and three segments of pericentrin in pcDNAI/Amp have been described previously (29, 30). HA-tagged Pc1–104 of pericentrin is constructed using HA-tagged full-length pericentrin, by cleaving the rest of the DNA and retaining only the first 104 amino acids of pericentrin. The cDNAs encoding the wild-type PKC βII, PKC βII K371R, and PKC βII T500E were subcloned into the pcDNA3 vector for expression in mammalian cells (31). The pseudosubstrate region (N-PS, residues 1–31) and the C1A domain (C1A, residues 32–111; N-C1A, residues 1–111) were expressed as glutathione *S*-transferase (GST) fusion proteins in mammalian cells following PCR amplification of the relevant sequences using pcDNA3-PKC βII as the template. Specifically, the primers used for the PCR amplification introduced a BamHI site and a ClaI site at the 5′ and 3′ ends, respectively. The PCR products were subcloned into the pEBG vector digested with BamHI and ClaI. The cDNA encoding the PKC-binding region of pericentrin (residues 454–593) was amplified by PCR and inserted into the EcoRI (5′ site) and the BamHI site (3′ site) of pEGFP-N1 (Clontech).

In Vitro Pull-down Assay—The DNA fragment corresponding to amino acids 454–593 of pericentrin (Pc454–593) was cloned into pGEX-KG (Amersham Biosciences), and GST fusion proteins were expressed in *E. coli* BL21, purified, and immobilized on glutathione-Sepharose beads (Amersham Biosciences) as described in the Amersham Biosciences instruction manual. 0.5 μg of pure PKC βII was incubated with 0.5 μg of fusion protein immobilized on glutathione-Sepharose beads in PBS buffer, pH 7.4, plus 1% Triton X-100 overnight at 4 °C with gentle rocking. Beads were then washed twice with the incubation buffer plus 500 mM NaCl and twice with the incubation buffer. Bound proteins were eluted with sample buffer, analyzed by SDS-PAGE and immunoblotting.

To examine the pericentrin-binding domain in PKC βII *in vitro*, the regulatory and catalytic domains of PKC were generated by incubation of purified PKC βII (2.5 μg/ml) with trypsin (2 units/ml) for 10 min at 30 °C in the incubation buffer with 1 mM $CaCl_2$. The purified PKC βII protein pretreated with or without trypsin was incubated with GST or GST fusion protein of pericentrin (GST-Pc454–593) immobilized on glutathione-Sepharose at 4 °C for 1 h in the presence of trypsin inhibitor (1 mg/ml). After being washed three times with the incubation buffer plus 300 mM NaCl, the proteins that bound to the glutathione beads were separated by SDS-PAGE and probed by the polyclonal anti-PKC βII antibody to detect full-length PKC βII and the catalytic domain and by the monoclonal anti-PKC β antibody to detect the regulatory domain of PKC βII.

Cell Culture and Transfection—HEK tsA201 and COS-7 cells were maintained in Dulbecco's modified Eagle's medium (Invitrogen) containing 10% fetal bovine serum (Invitrogen) at 37 °C in 5% CO_2. RIE-1 cells were maintained in Dulbecco's modified Eagle's medium containing 5% fetal bovine serum and 10 μg/ml purimycin. U2OS cells were grown in Dulbecco's modified Eagle's medium containing 10% fetal calf serum. For biochemical studies, transient transfection of tsA201 cells and COS-7 cells were carried out using Superfect transfection reagents (Qiagen). The specific transfection procedures were performed according to the protocol suggested by Qiagen. Combinations of the different expression plasmids were used as stated, and 1 μg of each construct DNA was generally included in the transfection. For immunofluorescence studies, COS-7 cells were grown on 12-mm round glass coverslips in 35-mm culture dishes and transfected with 1 μg of plasmid DNA (GFP vector, GFP-Pc454–593, HA-Pc454–593, HA-Pc1–104, pEBG-Pc494–593, or no DNA) using LipofectAMINE and LipofectAMINE Plus reagents (Invitrogen); transfection efficiency was ~30–50%. Cells were fixed at 17, 42, and 66 h after transfection and processed for immunofluorescence staining. All of the transfected cells were recognized by using antibodies against respective tags of the overexpressing protein. Cell growth was determined by measuring the ratio of transfected cells to the total cell population; there was little change in this ratio over a 62-h time period. In all quantitative studies, only transfected cells were counted and presented as percentage of transfected cells.

In Vivo GST Fusion Protein Pull-down Assay—To map the binding region of PKC βII to pericentrin *in vivo*, the N-PS region (residues 1–31), the N-C1A region (residues 1–111), and the C1A domain (residues 32–111) of PKC βII were expressed as GST fusion proteins in tsA201 cells together with HA-tagged pericentrin. Approximately 40 h post-transfection, the transfected cells were lysed in buffer A (20 mM HEPES, pH 7.4, 20 mM NaCl, 5 mM EDTA, 5 mM EGTA, 0.5% Triton X-100, 1 mM dithiothreitol, 2 mM benzamidine, 10 μg/ml leupeptin, 1 mM phenylmethylsulfonyl fluoride, and 100 nM microcystin-LR). The lysate was cleared by centrifugation at 13,000 rpm for 5 min at 22 °C, and the resulting supernatant is referred to as the detergent-solubilized cell lysate. 5% of the total cell lysate was kept in SDS sample buffer for further analysis, and the remaining whole cell lysate was incubated with glutathione-Sepharose at 4 °C for overnight. After washing twice in buffer B (buffer A plus 500 mM NaCl) and twice in buffer A, the glutathione-Sepharose-bound proteins were analyzed using SDS-PAGE and immunoblotting.

Immunoprecipitation—tsA201 cells were transiently transfected with different combinations of indicated constructs. About 40 h post-transfection, the cells were lysed in buffer A. 5% of the total detergent-solubilized cell lysates were kept in SDS sample buffer for further analysis, and the remaining detergent-solubilized cell lysate was incubated with appropriate monoclonal antibody and protein A/G-agarose at 4 °C overnight. The immunoprecipitates were washed twice in buffer B and twice in buffer A. The proteins in the immunoprecipitates were separated using SDS-PAGE and analyzed using immunoblotting.

Immunofluorescence Microscopy—Nontransfected cultured cells were rinsed in PBS, extracted with permeabilization buffer (20), and fixed in methanol at −20 °C. Transfected cells were fixed in methanol at −20 °C as described previously (20). Cells were observed under an Olympus IX-70 fluorescent microscope and imaged using a CoolSnap HQ CCD camera (Roper Scientific). Optical sections were taken, and the images were deconvolved (Metamorph; Universal Imaging Corp.). Immunofluorescence images are two-dimensional projections of three-dimensional reconstruction to ensure that all stained material is visible.

Flow Cytometry—For PKC βII mislocalization studies, U2OS cells were transfected with pEGFP (GFP) or pEGFP-Pc454–593 (GFP-Pc454–593) constructs using LipofectAMINE and LipofectAMINE Plus reagents (Invitrogen). Cells were processed for live cell sorting at 34 h post-transfection. GFP-positive cells were sorted by FACStar plus (Becton Dickinson). Sorted cells were plated on 12-mm round glass coverslips in 24-well plates. Cells were incubated overnight at 37 °C to facilitate attachment to the coverslip. Cells were permeabilized (20) and fixed in −20 °C methanol. Some cells were fixed without extraction to estimate the purity of the GFP-positive cells. Purity of the GFP-positive cells ranged from 95 to 98%. Fixed cells were processed for immunofluorescence staining. Only G_2/M stage cells were scored for the analysis. Cells that had duplicated and separated centrosomes were considered as G_2/M stage cells.

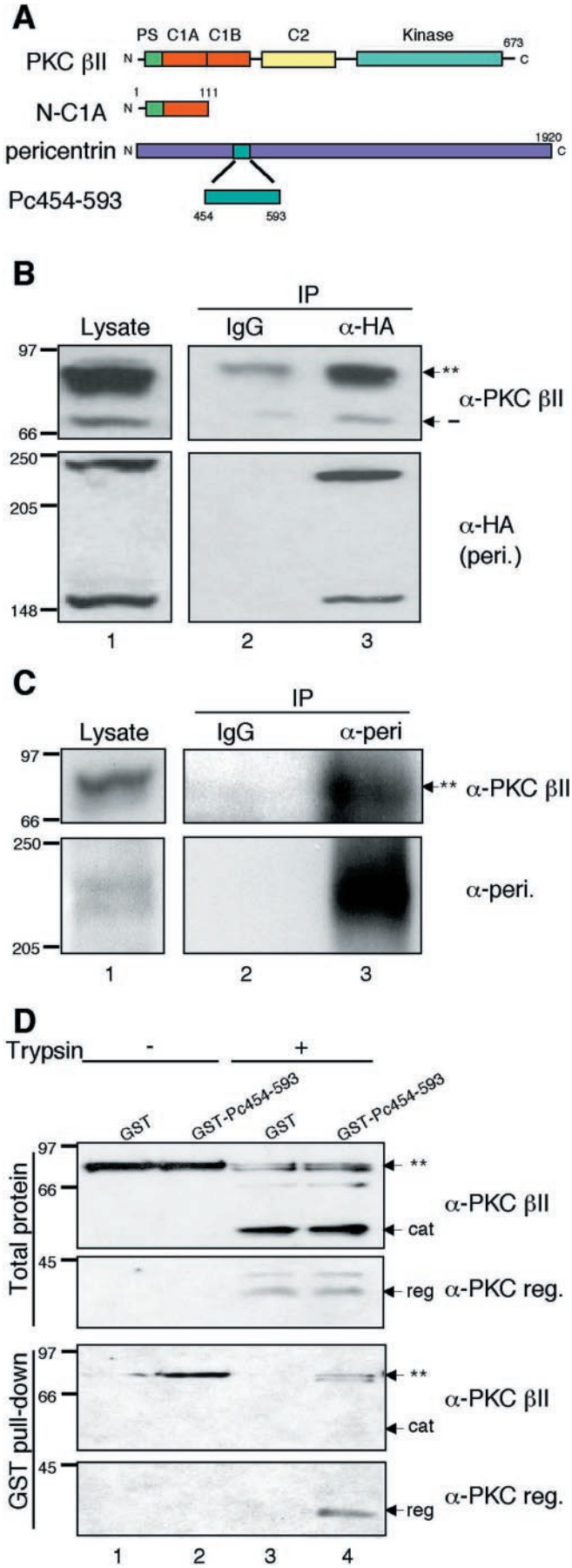

FIG. 1. **Identification of pericentrin as a novel PKC-binding protein.** *A*, the N-terminal region (residues 1–111) of PKC βII, shown schematically, was cloned into pAS2.1 vector and used as bait in a yeast two-hybrid screen using a mouse embryonic cDNA library. One of the positives was a cDNA fragment of 420 bp corresponding to residues 454–593 in pericentrin. *B*, Western blot showing PKC βII and HA-pericentrin in the detergent-solubilized lysate of tsA201 cells co-expressing both proteins (*lane 1*). Pericentrin (*peri.*) was immunoprecipitated (*IP*) from the detergent-solubilized lysate using an anti-HA antibody, and the immunoprecipitate was probed for PKC βII (*lane 3*); control IgG was used in control immunoprecipitation (*lane 2*). An *asterisk* indicates fully phosphorylated PKC, and a *dash* indicates unphosphorylated PKC. *C*, Western blot of detergent-solubilized lysate of K562 cells probed with anti-PKC βII antibody or anti-pericentrin antibody (*α-peri.*), UM225 (*lane 1*). Endogenous pericentrin was immunoprecipitated from the detergent-solubilized lysate using UM225 and probed for PKC βII (*lane 3*); preimmune sera were used in control immunoprecipitation (*lane 2*). *D*, pericentrin directly binds to the regulatory domain of PKC *in vitro*. Purified PKC βII (2.5 μg/ml) pretreated with or without trypsin (2 units/ml) was incubated with GST or a GST fusion protein of pericentrin (GST-Pc454–593) and then immobilized on glutathione-Sepharose at 4 °C for 1 h. Bound proteins were separated by SDS-PAGE and probed with a polyclonal antibody that detects the catalytic domain of PKC (*anti-Cat*) or a monoclonal antibody that detects the regulatory domain of PKC (*anti-Reg*). Western blot showing total protein (*upper panel*) or GST pull-down (*lower panel*) for PKC incubated with GST alone (*lanes 1* and *3*) or with GST-Pc454-593 (*lanes 2* and *4*) and then treated without (*lanes 1* and *2*) or with (*lanes 3* and *4*) trypsin. The position of full-length and fully phosphorylated PKC is indicated with a *double asterisk*; the positions of catalytic domain (*Cat*) and regulatory domain (*Reg*) are also indicated.

Time Lapse Imaging—COS-7 cells were plated on 35-mm glass bottom culture dishes (MatTek Corp, MA) and transfected with GFP-Pc454–593 or HA-Pc454–593. 22–24 h post-transfection, cells were placed in a chamber (PDMI-2; Harvard Apparatus) in complete medium with CO_2 exchange (0.5 liters/min) at 37 °C. Cells were imaged every 5 min for 20–22 h using a ×20 or ×30 phase-contrast lens on an inverted microscope (Olympus IX-70). Images were captured on a CoolSnap HQ CCD camera (Roper Scientific) and concatenated using Metamorph software (Universal Imaging Corp.).

Microtubule Regrowth Assay—The depolymerization of microtubules by nocodazole (10 μg/ml) treatment and regrowth of microtubules in COS-7 cells were performed as described previously (29). Cells were fixed in methanol at −20 °C and processed for immunofluorescence as described previously (20).

RESULTS

Identification of Pericentrin as a Novel Protein Kinase C-binding Protein—To identify novel PKC-binding proteins, we screened a mouse embryonic cDNA library with a fragment encoding the first 111 amino acids of PKC βII as bait. This sequence encodes the N-terminal tail, the pseudosubstrate sequence, and C1A domain of PKC (Fig. 1*A*; N-C1A). Approximately 100,000 clones were screened, with five positive clones obtained. Of these, one contained a 420-bp cDNA fragment encoding a 140-residue peptide corresponding to amino acids 454–593 of the centrosomal protein, pericentrin (Fig. 1*A*; Pc454–593).

To address whether PKC interacts with pericentrin *in vivo*, we co-transfected tsA201 cells with PKC βII and HA-tagged pericentrin. Pericentrin was immunoprecipitated from the detergent-solubilized fraction of cell lysates using anti-HA antibody, and the immunoprecipitate was analyzed for bound PKC βII by Western blot analysis. Analysis of cell lysates showed that recombinant pericentrin migrated as two bands of apparent molecular mass of 150 and 220 kDa on SDS-PAGE, as detected using either anti-pericentrin antibodies (data not shown) or anti-HA antibodies (Fig. 1*B*, *lower panel*, *lane 1*). The lower band is truncated at the C terminus (retains HA tag), as previously observed (29), and may reflect proteolysis or a partial transcript of pericentrin. Two species of PKC were also apparent in the lysates (Fig. 1*B*, *upper panel*, *lane 1*): a major slower migrating band (indicated by an *asterisk*) that represents fully phosphorylated PKC and a minor faster migrating species (labeled with a *dash*) that represents unphosphorylated

PKC (32). Both species were present in immunoprecipitates of pericentrin (Fig. 1*B*, *upper panel*); there was no apparent enrichment of either species of PKC in the immune complex. Control immunoprecipitates in which lysate was incubated with protein A/G-Sepharose had barely detectable amounts of bound PKC (*lane 2*). Conversely, we found that HA-pericentrin (also both bands) associated with immunoprecipitated PKC from tsA201 cells co-transfected with PKC and pericentrin (data not shown). These data reveal that PKC and pericentrin form a complex in cells.

We next asked whether endogenous pericentrin and endogenous PKC interact *in vivo*. We examined K562 cells because PKC βII is relatively abundant in these cells (33). Western blot analysis revealed that PKC βII migrated as a single band (Fig. 1*C*, *lane 1*); unlike the overexpressed protein, native protein was fully processed by phosphorylation. Fig. 1*C* shows that a polyclonal antibody to pericentrin, UM225, labeled a ~220-kDa band corresponding to pericentrin (20) and effectively immunoprecipitated the protein. PKC βII was present in the immune complex (*lane 3*) but was not associated with control beads incubated without antibody (*lane 2*).

To examine whether PKC binds pericentrin directly, we performed an *in vitro* GST pull-down assay using recombinant PKC βII purified from baculovirus-infected insect cells and either GST alone or a GST fusion protein of pericentrin 454–593 (GST-Pc454–593) purified from bacteria. In addition, to test which domain of PKC mediates its binding to pericentrin, we treated purified PKC βII with trypsin to generate the regulatory and catalytic moieties (38 and 50 kDa, respectively) of PKC, prior to incubation with the GST fusion proteins (Fig. 1*D*, *lanes 3* and *4*). Proteins bound to glutathione-Sepharose beads were identified by Western blot analysis using antibodies against the regulatory or catalytic domains of PKC. Fig. 1*D* shows that PKC βII bound to GST-Pc454–593 (*lane 2*) but not to GST alone (*lane 1*). Trypsin treatment of PKC yielded a 50-kDa catalytic fragment and 38-kDa regulatory fragment (*upper panel*, *lanes 3* and *4*). Only the regulatory fragment was precipitated by GST-Pc454–593 (*lower panel*, *lane 4*). These results indicate that PKC binds to pericentrin directly and that the binding determinants are located in its regulatory domain.

The C1A Domain of Protein Kinase Mediates the Interaction with Pericentrin—The bait we used in the yeast two-hybrid screen comprised the first 111 amino acids of PKC including the pseudosubstrate sequence and C1A domain. To further delineate the docking site for pericentrin in PKC, we expressed a series of GST-tagged constructs of the amino terminus of PKC: N-PS (first 31 residues containing the pseudosubstrate); C1A (residues 32–111, which comprise the C1A domain); and N-C1A (first 111 residues up to and including the C1A domain). HA-pericentrin was co-expressed with these GST-tagged constructs in tsA201 cells, the expressed GST-fusion proteins were immobilized to glutathione-Sepharose beads, and the bound proteins were analyzed by using anti-HA antibody to detect pericentrin (Fig. 2). The expression level of pericentrin was comparable in all of the cells transfected with different constructs (Fig. 2, *upper panel*). All GST-tagged constructs were expressed in tsA201 cells (Fig. 2, *upper panel*) and effectively precipitated by glutathione-Sepharose beads (Fig. 2, *lower panel*) as judged by staining with anti-GST antibodies. Pericentrin was associated with both of the PKC constructs that contained the C1A domain: GST-C1A (*lane 3*) and GST-N-C1A (*lane 4*). It did not interact with the construct lacking the C1A domain, GST-N-PS (*lane 2*); nor did it interact with the isolated C1B domain (data not shown). These data suggest that the C1A domain in the regulatory moiety of PKC provides the primary determinants in the interaction of PKC with pericentrin.

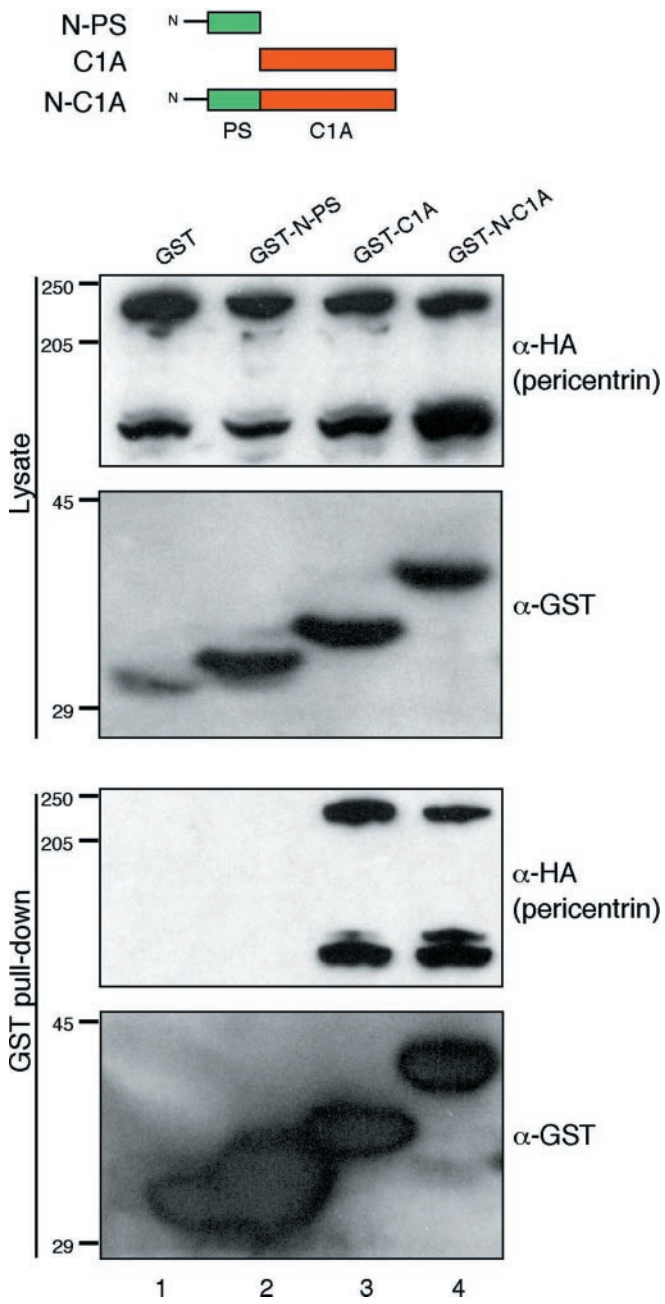

FIG. 2. **The C1A domain of PKC binds pericentrin *in vivo*.** The indicated GST-tagged fusion proteins encoding different regions of the regulatory moiety of PKC βII were co-expressed with HA-tagged pericentrin in tsA201 cells: GST vector, GST-N-PS, GST-C1A, and GST-N-C1A. Detergent-solubilized cell lysates were incubated with glutathione-Sepharose to precipitate the GST fusion proteins. *Upper panel*, Western blot showing total expression of pericentrin (probed with anti-HA antibody) or fusion constructs (probed with anti-GST antibody). *Lower panel*, Western blot showing pericentrin bound to beads and amount of fusion protein bound to beads.

PKC βII Is Localized to the Centrosome—The interaction of PKC βII with pericentrin suggested that pericentrin might anchor PKC at the centrosome (20). To test this possibility, we examined the subcellular localization of PKC βII by immunofluorescence microscopy using antibodies (C-18 from Santa Cruz Biotechnology) specific for the PKC βII isoform of the kinase (Fig. 3). PKC βII was localized to the centrosome in G_2 and mitotic cells. Centrosome localization was observed in U2OS cells (Fig. 3) and in RIE-1 and COS-7 cells (data not shown). Centrosome staining was observed in methanol-fixed cells and was enhanced following a brief pre-extraction of cells

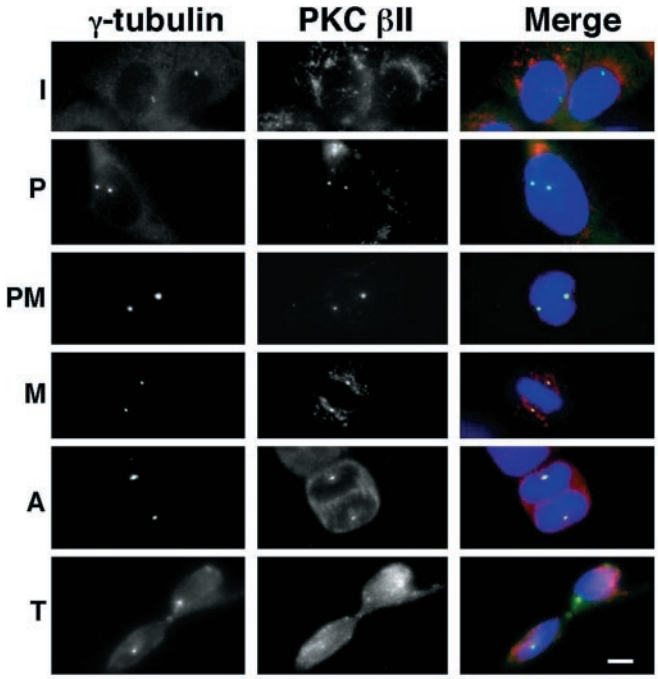

FIG. 3. **PKC βII is localized to the centrosome in G_2 and mitotic cells.** A micrograph shows staining of U2OS cells for γ-tubulin (*green*), PKC βII (*red*), and both together with 4′,6-diamidino-2-phenylindole (*DAPI*) (*blue*) to image DNA (*Merge*). Cell cycle stages are interphase (*I*), prophase (*P*), prometaphase (*PM*), metaphase (*M*), anaphase (*A*), and telophase (*T*). *Bar* (*bottom right panel*), 10 μm for *all panels*.

with detergent to reduce PKC βII staining at other cellular sites (29). During mitosis, the fluorescence intensity of PKC βII at the spindle poles/centrosomes increased from prophase to metaphase and then decreased to a minimum in telophase when it became more diffusely distributed in the cytoplasm (Fig. 3). This pattern was similar to that observed for pericentrin (21).

A PKC-binding Fragment of Pericentrin Disrupts the Interaction between PKC and Pericentrin in Vivo—To begin to explore the physiological relevance of the interaction of PKC with pericentrin, we tested whether peptide fragments of the interaction regions on the two proteins could disrupt the PKC-pericentrin interaction in cells. Specifically, we addressed whether the 140-residue fragment of pericentrin originally obtained from the yeast two-hybrid assay, Pc454–593, could disrupt the binding of PKC to pericentrin *in vivo*. tsA201 cells were co-transfected with pericentrin, PKC βII, and either vector alone or GFP-Pc454–593. Pericentrin was then immunoprecipitated from the detergent-solubilized fraction, and the amount of co-immunoprecipitated PKC was detected by Western blot analysis. The expression level of transfected PKC (Fig. 4*A*, *upper panel*) and pericentrin (Fig. 4*A*, *second panel*) was comparable whether or not GFP-Pc454–593 was co-expressed (Fig. 4*A*, *compare lanes 1* and *2*). Pericentrin was immunoprecipitated with comparable efficiency in the absence (*lane 1*, GFP vector) or presence (*lane 2*) of co-expressed GFP-Pc454–593. PKC βII was present in the immune complex with pericentrin (Fig. 4*A*, *HA IP*, *lane 1*). However, co-expression of GFP-Pc454–593 caused a marked reduction in the amount of PKC associated with pericentrin (*lane 2*). Quantification of the results from four independent experiments revealed a 4.0 ± 0.7-fold reduction in bound PKC in the presence of GFP-Pc454–593. Thus, Pc454–593 effectively disrupts the interaction of PKC and pericentrin *in vivo*.

Disruption of the Pericentrin-PKC βII Interaction in Vivo Releases PKC βII from Centrosomes—The biochemical data

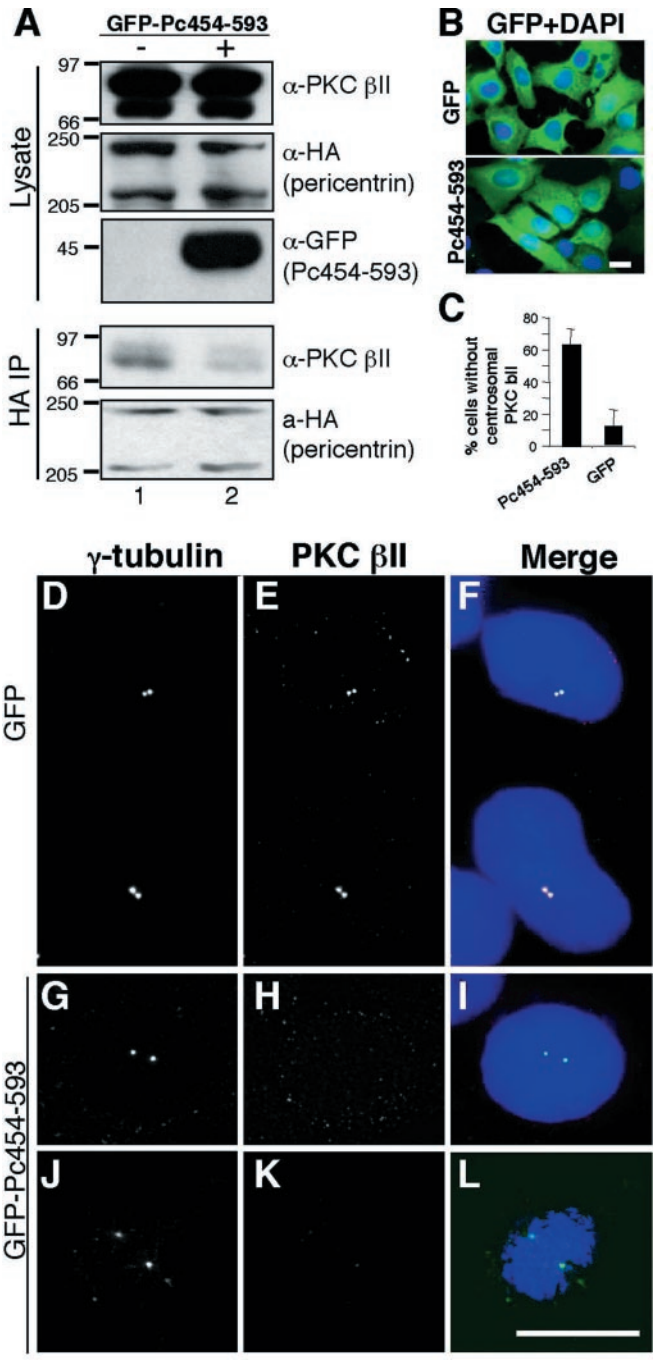

FIG. 4. **Disruption of the pericentrin-PKC βII interaction by co-expression of GFP-tagged PKC-binding region (GFP-Pc454–593) of pericentrin.** *A*, tsA201 cells were transiently transfected with HA-pericentrin and PKC βII together with vector or GFP-Pc454–593. Pericentrin was immunoprecipitated from detergent-solubilized cell lysates with the anti-HA antibody coupled to protein A/G-agarose. Western blot shows expression of PKC βII, pericentrin, and GFP-Pc454–593 in the detergent-solubilized lysate of cells transfected without (*lane 1*) and with GFP-Pc454–593 (*lane 2*) in the *upper panels*, and the *lower panels* show the presence of pericentrin and PKC βII in the corresponding immunoprecipitates. *B*, U2OS cells were transiently transfected with GFP-Pc454–593 or GFP. GFP-positive cells are sorted and extracted. Extracted cells were stained with anti γ-tubulin antibody (*D*, *G*, and *J*), PKC βII (*E*, *H*, and *K*), and 4′,6-diamidino-2-phenylindole (*DAPI*). G_2 stage cells were scored in both GFP-Pc454–593- and GFP-overexpressing cells. GFP-Pc454–593-expressing cells show mislocalization of PKC βII at their centrosomes (*H* and *K*). *F*, *I*, and *L* show the merge of γ-tubulin, PKC βII, and 4′,6-diamidino-2-phenylindole. Non-extracted cells (*B*) were stained with anti-GFP polyclonal antibody and 4′,6-diamidino-2-phenylindole to estimate the purity of the sorted cells. Cells were 95–98% GFP-positive. *Bar* in *L*, 10 μm for *D–L*; and *bar* in *B*, 10 μm for *B*.

showing that the PKC βII-interacting fragment of pericentrin could uncouple the pericentrin-PKC βII interaction suggested that this peptide fragment might also dissociate the kinase from the centrosome if it is anchored there by pericentrin. To test this, cells expressing GFP-Pc454–593 or GFP alone were isolated by flow cytometry, replated, and analyzed for localization of endogenous PKC βII to centrosomes. Nearly all sorted cells (95–100%) expressed GFP-Pc454–593 or GFP alone (Fig. 4*B*). Over 60% of GFP-Pc454–593-overexpressing cells in G_2 or mitosis had undetectable levels of PKC βII at centrosomes (Fig. 4, *C* and *G–L*) compared with control cells overexpressing GFP alone (Fig. 4, *C–F*). Under the same conditions, we observed no detectable change in centrosome localization of pericentrin (data not shown) or γ−tubulin (Fig. 4, *H* and *J*). These data are consistent with a role for pericentrin in anchoring PKC βII at centrosomes in G_2 and mitotic cells.

Overexpression of the PKC-binding Domain of Pericentrin Induces Microtubule Defects, Cytokinesis Failure, Spindle Defects, and Chromosome Missegregation—We next examined the effect of disrupting the association of PKC βII with pericentrin and, thus, the centrosome. Cells expressing the PKC binding domain of pericentrin (Pc454–593) and control proteins were analyzed at several different times after transfection (Fig. 5*A*). At all times examined, most cells expressing control constructs (HAPc1–104) or nontransfected cells showed normal microtubule organization (88–91%). In these cells, the majority of microtubules were focused on centrosomes and organized into well defined radial arrays (Fig. 5, *A* and *B*). In contrast, profound changes in microtubule organization were observed in the majority of cells expressing Pc454–593 (over 80%) even at the earliest times examined (17 h post-transfection), when the levels of overexpressed proteins were low. Microtubules did not form radial arrays or converge on centrosomes but were more randomly organized in the cytoplasm (unfocused and disorganized microtubules) (Fig. 5, *C* and *D*) and often formed bundles that wrapped around the nucleus (whorled microtubules) (Fig. 5, *E* and *F*). This phenotype was also observed with a smaller pericentrin construct (Fig. 5*G*, Pc494–593). Although centrosomal microtubules were severely disorganized, microtubule nucleation from the centrosome was unaffected (data not shown), suggesting that microtubule anchoring rather than nucleation was perturbed. The structural integrity of the centrosome appeared normal, since other centrosome proteins localized normally to centrosomes including γ-tubulin (34), pericentrin, α-tubulin (centrioles), dynein (29), and several recognized by the human autoimmune serum 5051 (Fig. 5, *B*, *D*, and *F*; data not shown).

As observed in interphase, mitotic cells overexpressing Pc454–593 exhibited defects consistent with microtubule disorganization at centrosomes/spindle poles (80%, $n = 26$) (Fig. 6). Astral microtubule arrays were markedly reduced (Fig. 6, *C–H*, *K*, and *L*); centrosomes were detached from central spindles (Fig. 6, *C* and *D*, *arrowheads*); and spindle poles were disorganized, flattened, or apparently fragmented (Fig. 6, *E–H*). In telophase cells, microtubules were not organized around centrosomes (Fig. 6, *K–M*) as in controls (Fig. 6*I*), and they often failed to form discrete central spindles and midbodies (Fig. 6*J*) typical of control cells (Fig. 6, *I* and *M*). DNA was often observed within intercellular bridges, and chromosomes were missegregated (Fig. 6, *K* and *M*), resulting in nuclei of variable size (Fig. 6, *K* and *L*, *upper insets*). Abnormal partitioning of the cytoplasm generated cells of dramatically different sizes (Fig. 6*L*). Taken together, these results demonstrate that disorganized microtubules in both interphase and mitotic cells contribute to defects in spindle organization, cytokinesis, and chromosome segregation, possibly through loss of microtubule anchoring at centrosomes and spindle poles.

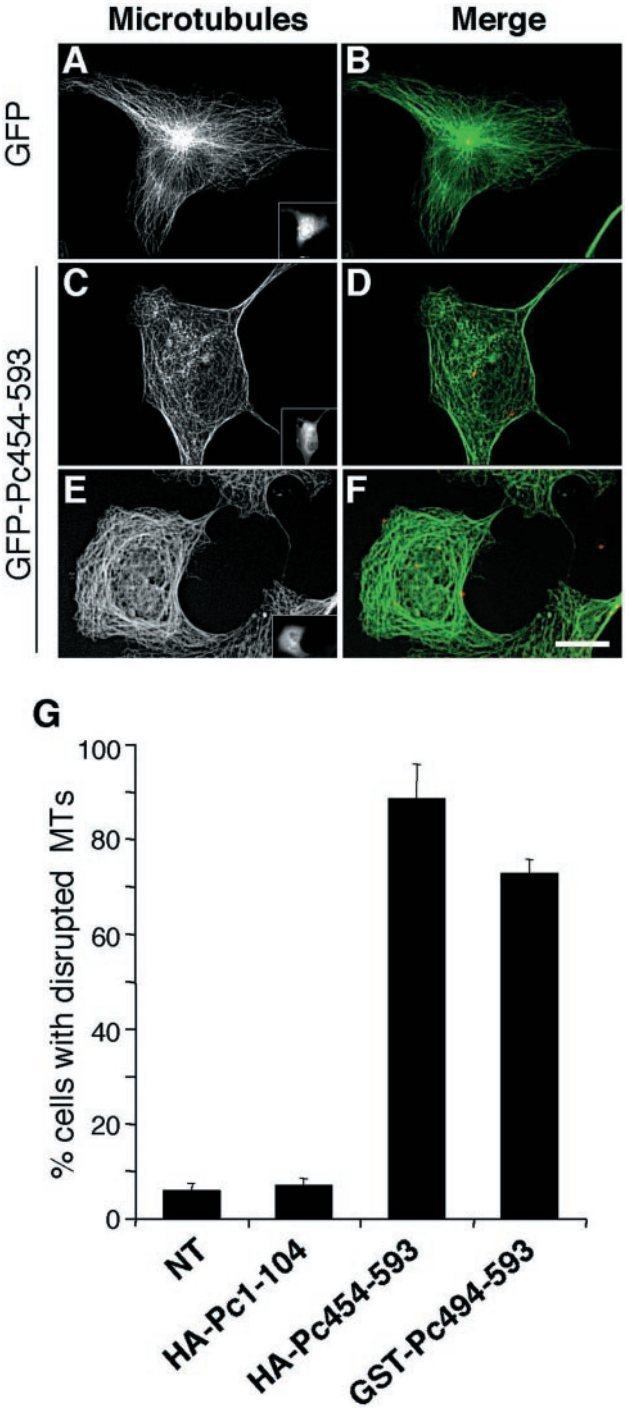

FIG. 5. **Microtubules are disorganized in interphase cells overexpressing the PKC-binding domain of pericentrin (Pc454–593).** *A–F*, COS-7 cells overexpressing the PKC-binding domain of pericentrin fused to GFP (GFP-Pc454–593; *insets* of *C* and *E*) or GFP alone (GFP vector control; *inset* of *A*). Cells were stained with 5051 serum to detect centrosomes (*red*) and microtubules (*blue*, *pseudocolored green*). Microtubules in control cells are focused at the centrosome (*B*), whereas those in GFP-Pc454–593-expressing cells are disorganized and lose their attachment to the centrosome (disorganized MTs; *D*) or wrapped around the nucleus (whorled MTs; *F*). *Bar* in *F*, 10 μm for *A–F*. *G*, quantification of microtubule disorganization (disorganized and whorled microtubules) in cells expressing the HA-Pc454–593, HA-Pc1–104, or a 100-amino acid PKC-binding domain of pericentrin fused to GST (GST-Pc494–593) or in nontransfected cells (*NT*). *Bars* represent data from at least 500 cells from three independent experiments.

Another early effect of overexpressing the PKC βII-interacting domain of pericentrin (17 h post-transfection) was a dra-

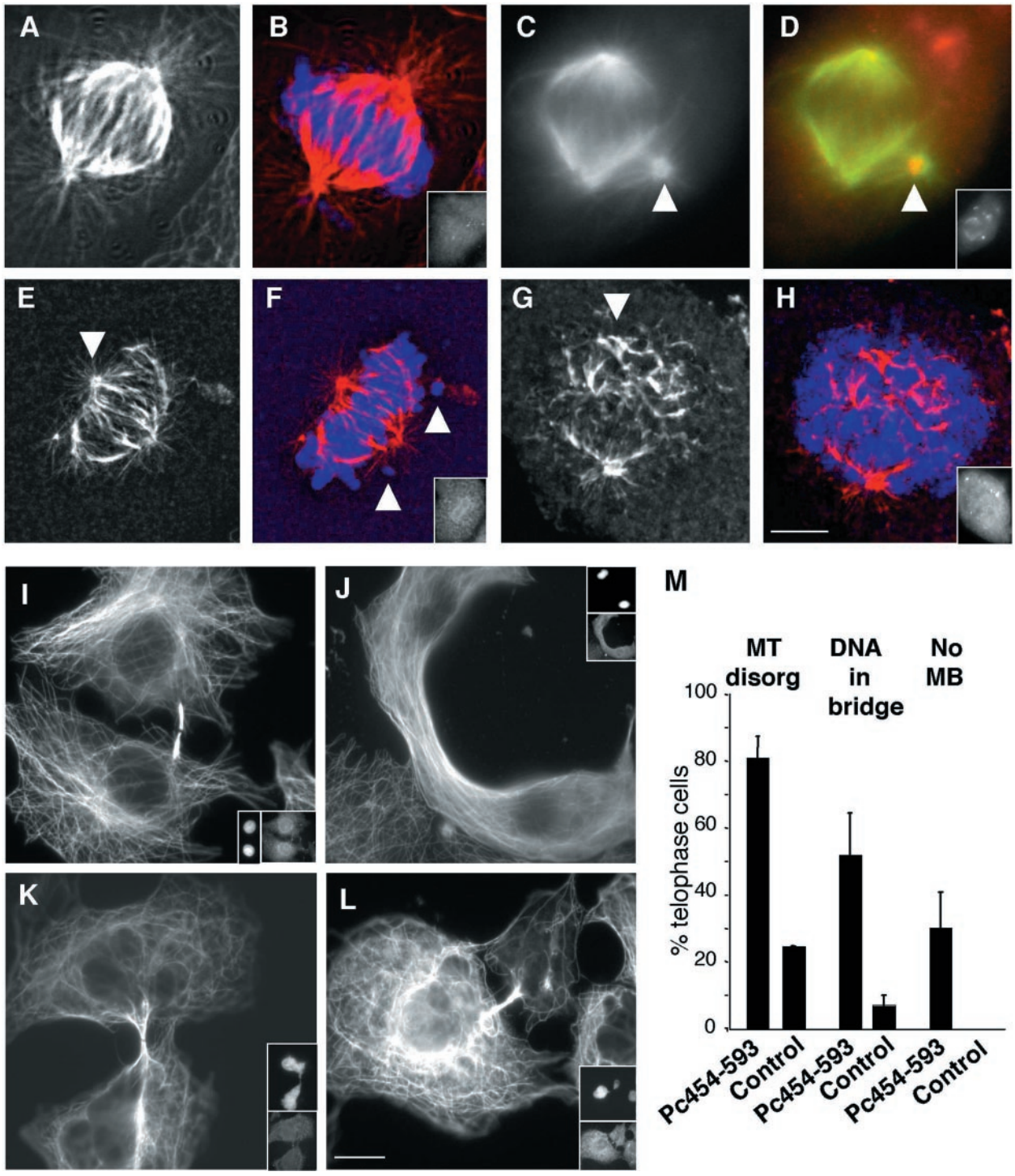

FIG. 6. **Microtubule organization is disrupted in mitotic cells overexpressing the PKC-binding domain of pericentrin (Pc454–593).** *A–H*, microtubule defects in metaphase COS-7 cells expressing HA-Pc454–593; *C–H*, loss of centrosomes from spindle poles; *C* and *D*, loss of spindle architecture (*arrowheads*, *E* and *F*), spindle pole disruption (*arrowhead*, *G* and *H*), and misaligned chromosomes (*arrowheads*, *E* and *F*) compared with normal spindles in control cells expressing HA-Pc1–104 (*A* and *B*). In all pairs, microtubules are shown in the first image (*A*, *C*, *E*, and *G*) and merged with DNA (*B*, *F*, and *H*) or centrosome marker, 5051 (*D*). *Insets* in the *bottom right corner* show overexpressed HA-tagged protein. *Bar* in *H*, 10 μm for *A–H*. *I–M*, defects in telophase cells expressing HA-Pc454–593 include wide intercellular bridges with microtubule bundles (*J*), disorganized centrosomal microtubules (*K* and *L*), undetectable midbody (*J–L*), DNA within bridge (*K* and *L*, *insets*, *top*), and unequal division of DNA and daughter cell cytoplasm (*L*) compared with normal structures in HA-Pc1–104-expressing cells (*I*). *Insets* show nuclei (*top* in *J–L*, *left* in *I*) and HA-tagged proteins (*bottom* in *J–L*, *right* in *I*). *Bar* in *L*, 10 μm for *I–L*. Quantification of results is shown in *M*. *MT disorg*, microtubule disorganization; *MB*, midbody. Each *bar* shows average of three experiments and a total of >70 cells per *bar*.

matic increase in the percentage of telophase cells in the total cell population compared with control cells (Fig. 7*A*). Time lapse imaging of living cells revealed significant delays and defects in telophase (Fig. 7*C*) compared with control cells (Fig. 7*B*). Cells appeared to progress through the early stages of mitosis and cytokinesis without significant difficulty but were delayed at later stages. Most showed a partially constricted cleavage furrow that changed in length and diameter throughout the period of frustrated cytokinesis (Fig. 7*C*, *arrowhead*). In many cases, the cleavage furrow regressed to produce large

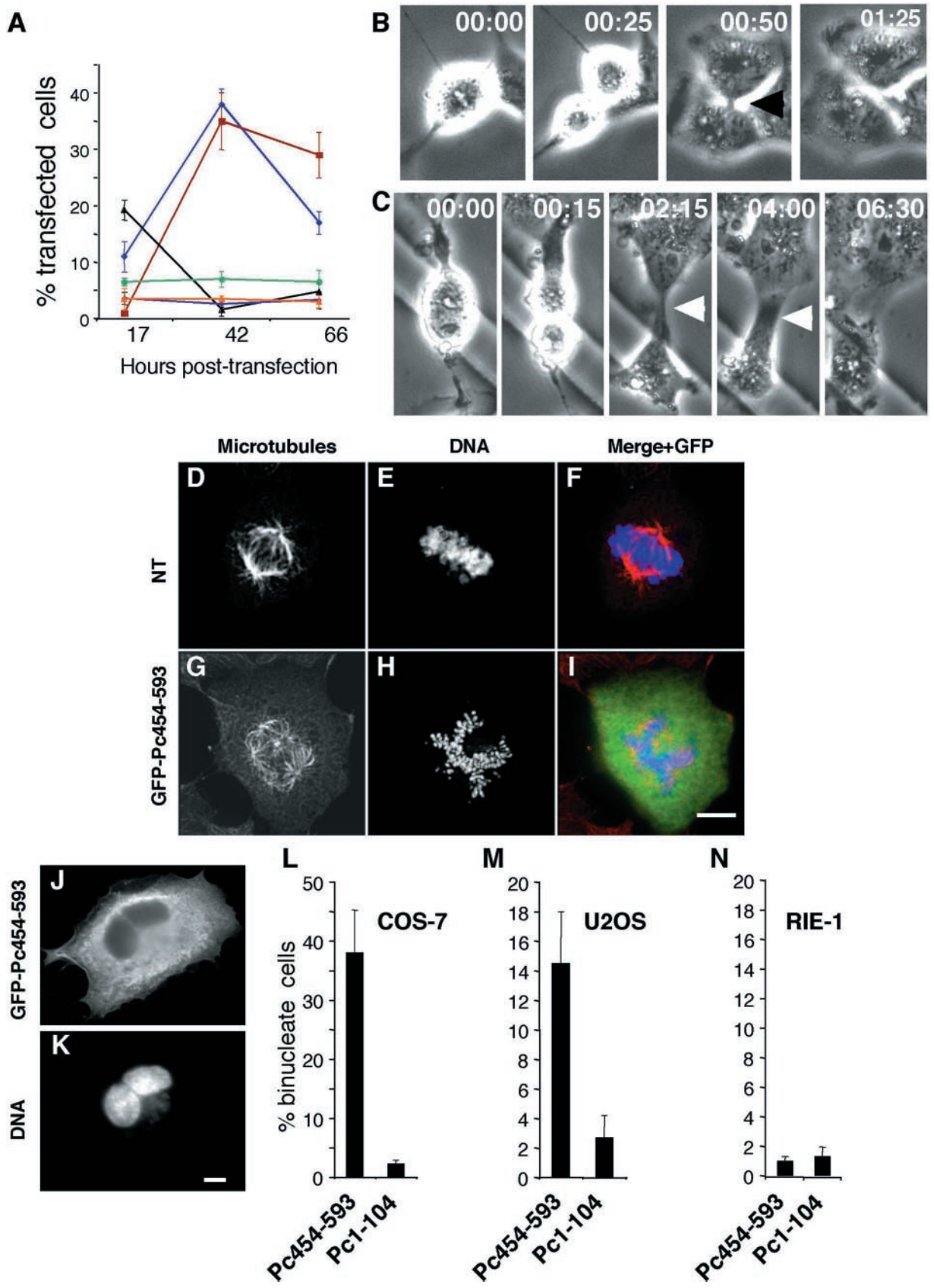

FIG. 7. **Cytokinesis delays and defects are induced in cells expressing Pc454–593.** *A*, graphs showing that microtubule defects are highest at early times post-transfection, whereas binucleate cells and multipolar spindles peak later. Pc454–593-expressing COS-7 cells are shown as follows: telophase cells (*black triangles*), binucleates (*blue diamonds*), and multipolar spindles (*brown squares*). Pc104-expressing cells are as follows: telophase (*orange triangles*), binucleates (*navy blue diamonds*, *lower line*), and multipolar spindles (*green circles*). Cells counted for each bar are as follows: telophase ($n > 500$), binucleates ($n > 500$), and multipolar spindles ($n = 25–50$). *B* and *C*, time lapse images of a Pc454–593-expressing COS-7 cell (*C*) showing a persistent intercellular bridge during a protracted period of cytokinesis without cleaving (*arrowhead*), compared with a control Pc104-expressing cell that undergoes a normal division within 85 min and shows a normal constricted

cells with two nuclei and two centrosomes. Consistent with observations in living cells, binucleate cells were also observed in fixed cell preparations in cells expressing the disrupting domain of pericentrin (Fig. 7, *A*, *J*, and *K*). Binucleate cell formation appeared to be specific for cells that express PKC βII (COS-7 and U2OS) (Fig. 7, *L* and *M*) and was not observed in cells that lack this isoform (rat intestinal epithelial cells, RIE-1) (Fig. 7*N*) (35). Moreover, cells lacking PKC βII showed no changes in microtubule organization or cytokinesis upon expression of the PKC βII-interacting domain of pericentrin (data not shown). These data suggest that a specific interaction between pericentrin and PKC βII controls progression through cytokinesis.

At later times after transfection (42–66 h), binucleate cells increased dramatically (Fig. 7*A*) while the population of telophase cells declined to control levels (Fig. 7*A*). This demonstrated that cytokinesis delays and defects preceded the increase in binucleate cell formation. Multipolar spindles also appeared at later times (Fig. 7, *A* and *G–I*), apparently arising from excess centrosomes generated by cytokinesis failure. Consistent with this idea was the observation that 97% of all defective spindles were multipolar compared with earlier time points (5%). This temporal analysis suggested that microtubule defects induced cytokinesis failure, which in turn produced binucleate cells, supernumerary centrosomes, and mutlipolar spindles.

Overexpression of the Pericentrin-binding Domain of PKC βII C1A or Dominant Negative Forms of the Kinase Induce Phenotypes Indistinguishable from Those Caused by Overexpression of Pc454–593—The data presented thus far do not rule out the possibility that expression of the PKC βII binding domains of pericentrin (Pc454–593 and Pc494–593) affected molecules other than PKC βII. To address this possibility, we asked whether the phenotype produced by the pericentrin domains could be reproduced using the C1A domain of PKC βII or a dominant-negative form of the kinase. Both proteins induced microtubule disorganization (unfocused microtubules and whorled microtubules) (Fig. 8*A*) and cytokinesis failure (Fig. 8*B*) at levels similar to those observed in Pc454–593-expressing cells. Cells lacking PKC βII (RIE) did not show these defects (data not shown). In addition, wild-type PKC βII caused cytokinesis failure (Fig. 8*B*), consistent with it acting as a dominant negative protein that is not phosphorylated or activated (see lower band in Fig. 1*B*) due to limitations in its processing by the upstream kinase, PDK-1. Indeed, the T500E construct of PKC βII, which bypasses the requirement for PDK-1 (31), did not cause a significant increase in binucleate cell production (data not shown).

Importantly, cytokinesis failure was not observed with other isoforms of the kinase. Overexpression of wild type or kinase-inactive PKC ε or ζ did not cause a significant increase in binucleate cell production over controls (Fig. 8*C*). Overexpression of wild type or kinase-inactive PKC α did not cause a significant increase in binucleate production (data not shown). These data suggest that kinase-inactive variants of PKC βII act as dominant negative inhibitors perhaps by disrupting the interaction of the endogenous enzyme with pericentrin to induce microtubule defects and cytokinesis failure. This idea was supported by the observation that the effects of PKC βII on microtubules and cytokinesis were partially reversed when the kinase was co-expressed with Pc454–593 (data not shown).

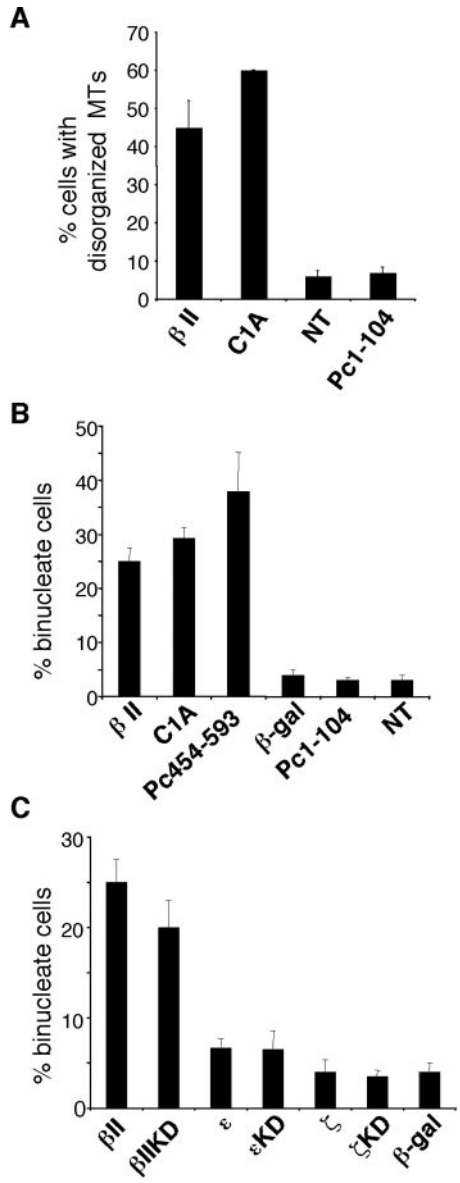

FIG. 8. **Kinase-inactive PKC βII and the C1A domain of PKC βII, but not other PKC isoforms, induce microtubule defects and cytokinesis failure.** *A*, quantification of disorganized microtubules (as shown in Fig. 5) in COS-7 cells expressing PKC βII, C1A, HA-Pc1–104, and nontransfected cells. The *bars* represent results from two independent experiments in which 200–500 cells were counted. *B* and *C*, quantification of binucleate cells expressing the wild-type PKC βII, kinase-inactive PKC βII (*βII KD*), PKC ε (ε), kinase-inactive PKC ε (ε *KD*), PKC ζ (ζ), kinase-inactive PKC ζ (ζ *KD*), and the GST-C1A domain of PKC βII (*C1A*) HA-Pc454–593, β-galactosidase (*β-gal*), HA-Pc1–104, and nontransfected cells (*NT*). Cells were analyzed for the presence of binucleate cells 42 h post-transfection. Data are expressed as the percentage of total cells that have more than one nucleus. At least 500 total cells were counted in three independent experiments.

DISCUSSION

In this study, we identified pericentrin as a scaffold protein that tethers PKC βII at the centrosome. This interaction is mediated by the C1A domain of PKC and a region within residues 454 and 593 of pericentrin. Disruption of this interac-

intercellular bridge (*B*, *arrowhead*). Time is represented as hours and minutes. *D–I*, images of spindles stained for α-tubulin (*D* and *G*) and DNA (*E* and *H*) and merged with GFP (*F* and *I*) in a GFP-Pc454–593-expressing cell (*G–I*) and a nontransfected cell (*D–F*). *Bar* in *I*, 10 μm for all. *J* and *K*, images showing a binucleate cell (*K*, DNA) transfected with Pc454–593 (*J*, GFP-Pc454–593). *Bar* in *K*, 5 μm for *J* and *K*. *L–N*, quantification of binucleate cells expressing the HA-Pc454–593 and Pc1–104 in COS-7 (*L*), U2OS (*M*), and RIE-1 (*N*) cells. RIE-1 cells do not express PKC βII and did not induce binucleate formation.

tion in cells releases PKC βII from centrosomes and results in microtubule disorganization, cytokinesis failure, spindle dysfunction, and aneuploidy.

Model for Control of Cytokinesis by PKC βII—Our data are consistent with a model in which cytokinesis failure is a direct consequence of microtubule disruption, which, in turn, is a direct consequence of displacing PKC βII from pericentrin. We propose a model to explain the cytokinesis defects induced by expression of the interacting domains of pericentrin and PKC βII. Specifically, expression of either of these disrupts the binding of PKC βII to pericentrin, which leads to a defect in microtubule organization at centrosomes and spindle poles. Impaired microtubule anchoring at these sites is supported by the pattern of disorganized microtubules and retention of microtubule nucleating activity. Poorly anchored microtubules are then likely to contribute to spindle dysfunction, leading to chromosome missegregation. Cytokinesis failure could result from disorganized microtubules at centrosomes and intercellular bridges or indirectly from chromatin that becomes trapped between nascent daughter cells. Excess centrosomes resulting from cytokinesis failure could organize multipolar spindles and promote additional chromosome missegregation. Although we favor this model, it is also possible that cytokinesis failure occurs by mechanisms other than microtubule disorganization that were not uncovered in this study. In any case, disruption of the pericentrin-PKC βII interaction clearly contributes to aneuploidy and perhaps other tumor-associated features that were first described in cells expressing full-length pericentrin (26, 29). The ability to generate aneuploid cells under these conditions may have important consequences in tumors where pericentrin levels are known to be elevated (26, 36, 37).

The mechanism for controlling cytokinesis by tethering PKC to the centrosome via pericentrin appears to be specific for cells expressing PKC βII. Whereas expression of the PKC-binding region of pericentrin causes severe morphological defects in cell lines expressing endogenous PKC βII, the RIE cell line that does not express this isozyme is not affected by overexpression of this disrupting domain. This degree of specificity is particularly remarkable given that RIE cells express the alternatively spliced PKC βI isozyme that differs only in the carboxyl-terminal segment (35). One possibility is that PKC βI is not localized to the centrosome because it is sequestered at other intracellular sites and hence is not sensitive to the pericentrin fragment. Alternatively, the carboxyl-terminal segment may contribute conformationally or structurally to the interaction of PKC βII, but not βI, with pericentrin. More broadly, these data suggest that alternative mechanisms for controlling cytokinesis operate in cells that do not express PKC βII. In support of a separate mechanism in cells that do not express PKC βII, introduction of PKC βII into RIE cells does not render them sensitive to effects of the pericentrin-disrupting fragment, Pc454–593. Whether other PKC isozymes serve a similar function in these cells remains to be explored. Such redundancy of function could account for the viability of mice deficient in PKC βII (38).

Cytokinesis Defects Are Induced by Elevating Levels of Other Centrosome-associated Kinases—The cytokinesis failure observed in this study is similar to that induced by overexpression of two other centrosome-associated kinases, aurora and polo, and suggests a functional link between aurora, polo, PKC, and pericentrin. Overexpression of aurora and polo induce the formation of binucleate cells at a level similar to that observed in this study (39, 40). Future studies will be required to determine whether the three kinases function independently or together as part of a pathway that ensures accurate partitioning of chromosomes into daughter cells. It is also interesting that all three kinases have been implicated in genetic instability and tumorigenesis (39–41).

Our data demonstrate that PKC βII is mislocalized from centrosomes in cells expressing the PKC βII binding domain of pericentrin, and they suggest that uncoupling of the kinase from pericentrin at this site is sufficient to induce cytokinesis failure.

PKC Is Implicated in Microtubule-dependent Processes, Cytokinesis, and Spindle Pole Body Duplication—Previous data have shown that PKC is involved in microtubule organization and centrosome positioning. Activated PKC isoforms have been shown to bind microtubules in T cells, U923 cells, and *Aplysia* neurons, and the results suggested that they may play a role in regulating microtubule dynamics or stability (19, 42, 43). A role for PKC in orienting the centrosome has also been suggested in studies of *Drosophila* embryos and T lymphocytes (44, 45). Several isoforms of PKC have been implicated in cytokinesis in yeast, *Aspergillus*, *Xenopus*, and vertebrates (46–51). Results from one *in vitro* study suggested that PKC was involved in actin ring formation and closure in *Xenopus* (50). However, most of these studies described the appearance of cells with excess DNA or extra nuclei but did not address the mechanism by which these aneuploid cells were generated. In this study, we define a series of cellular events induced by expression of dominant-negative forms of PKC βII that are initiated by loss of microtubule anchoring at centrosomes and ultimately lead to cytokinesis failure and aneuploidy. The requirement for catalytically competent PKC βII for normal cytokinesis suggests that docking to pericentrin poises this isozyme for access to a specific substrate. *In vitro* phosphorylation assays with pure PKC βII and pericentrin and *in vivo* labeling with [^{32}P]orthophosphate indicate that pericentrin is not the substrate (data not shown). Thus, whereas pericentrin has a key role in positioning PKC βII at the centrosome, the immediate target of pericentrin-tethered PKC βII remains to be identified.

PKC, Pericentrin, and Centrosome Duplication—Recent data suggest that at least two isoforms of pericentrin exist in vertebrate cells, pericentrin-220 and -350, and both localize to centrosomes (20, 23, 24). We have shown in this study that PKC βII binds both pericentrin isoforms (Fig. 1, *B* and *C*) (data not shown). A calmodulin-binding domain in pericentrin-350 is homologous to *Saccharomyces cerevisiae* Spc110, a component of the budding yeast spindle pole body (the centrosome equivalent) (23), suggesting that pericentrin-350 is an Spc110 orthologue. Recent work has shown that overexpression of the *S. cerevisiae* PKC1 rescues the growth-suppressive effect of a mutation in Spc110 (52). In addition, genetic interactions were identified between PKC1 and genes that control spindle pole body duplication. This led the authors to suggest that the PKC pathway regulates spindle pole body duplication perhaps by regulating the spindle pole body component Spc110. The role of PKC βII and pericentrin in spindle pole body duplication in vertebrate has not been examined.

Pericentrin as a Multikinase Scaffold—Pericentrin was previously identified as a scaffold for protein kinase A (53). Specifically, pericentrin contains a novel protein kinase A regulatory subunit II binding domain in a segment of the protein distinct from the segment that binds PKC. Disruption of this interaction induces spindle abnormalities in HEK 293 cells (54), similar to what we have observed when the interaction of pericentrin and PKC was disrupted. These findings raise the intriguing possibility that pericentrin might function as a multikinase scaffold that directs PKC, protein kinase A, and other signaling enzymes to the centrosome to modulate centrosomal and perhaps cellular functions.

REFERENCES

1. Newton, A. C. (1997) *Curr. Opin. Cell Biol.* **9,** 161–167
2. Nishizuka, Y. (1995) *FASEB J.* **9,** 484–496
3. Mochly-Rosen, D. (1995) *Science* **268,** 247–251
4. Kiley, S. C., Jaken, S., Whelan, R., and Parker, P. J. (1995) *Biochem. Soc. Trans.* **23,** 601–605
5. Black, J. D. (2000) *Front Biosci.* **5,** D406–D423
6. Livneh, E., and Fishman, D. D. (1997) *Eur. J. Biochem.* **248,** 1–9
7. Ashton, A. W., Watanabe, G., Albanese, C., Harrington, E. O., Ware, J. A., and Pestell, R. G. (1999) *J. Biol. Chem.* **274,** 20805–20811
8. Zezula, J., Sexl, V., Hutter, C., Karel, A., Schutz, W., and Freissmuth, M. (1997) *J. Biol. Chem.* **272,** 29967–29974
9. Thompson, L. J., and Fields, A. P. (1996) *J. Biol. Chem.* **271,** 15045–15053
10. Levin, D. E., Fields, F. O., Kunisawa, R., Bishop, J. M., and Thorner, J. (1990) *Cell* **62,** 213–224
11. Doxsey, S. (2001) *Nat. Rev. Mol. Cell. Biol.* **2,** 688–698
12. Jaken, S., and Parker, P. J. (2000) *BioEssays* **22,** 245–254
13. Correas, I., Diaz-Nido, J., and Avila, J. (1992) *J. Biol. Chem.* **267,** 15721–15728
14. Robinson, P. J. (1991) *Mol. Neurobiol.* **5,** 87–130
15. Kiley, S. C., and Parker, P. J. (1995) *J. Cell Sci.* **108,** 1003–1016
16. Kiley, S. C., and Parker, P. J. (1997) *Cell Growth Differ.* **8,** 231–242
17. Takahashi, M., Mukai, H., Oishi, K., Isagawa, T., and Ono, Y. (2000) *J. Biol. Chem.* **275,** 34592–34596
18. Volkov, Y., Long, A., and Kelleher, D. (1998) *J. Immunol.* **161,** 6487–6495
19. Volkov, Y., Long, A., McGrath, S., Ni Eidhin, D., and Kelleher, D. (2001) *Nat. Immunol.* **2,** 508–514
20. Doxsey, S. J., Stein, P., Evans, L., Calarco, P. D., and Kirschner, M. (1994) *Cell* **76,** 639–650
21. Dictenberg, J. B., Zimmerman, W., Sparks, C. A., Young, A., Vidair, C., Zheng, Y., Carrington, W., Fay, F. S., and Doxsey, S. J. (1998) *J. Cell Biol.* **141,** 163–174
22. Takahashi, M., Shibata, H., Shimakawa, M., Miyamoto, M., Mukai, H., and Ono, Y. (1999) *J. Biol. Chem.* **274,** 17267–17274
23. Flory, M. R., Moser, M. J., Monnat, R. J., Jr., and Davis, T. N. (2000) *Proc. Natl. Acad. Sci. U. S. A.* **97,** 5919–5923
24. Li, Q., Hansen, D., Killilea, A., Joshi, H. C., Palazzo, R. E., and Balczon, R. (2001) *J. Cell Sci.* **114,** 797–809
25. Gillingham, A. K., and Munro, S. (2000) *EMBO Rep.* **1,** 524–529
26. Pihan, G. A., Purohit, A., Wallace, J., Malhotra, R., Liotta, L., and Doxsey, S. J. (2001) *Cancer Res.* **61,** 2212–2219
27. Orr, J. W., Keranen, L. M., and Newton, A. C. (1992) *J. Biol. Chem.* **267,** 15263–15266
28. Vojtek, A. B., and Hollenberg, S. M. (1995) *Methods Enzymol.* **255,** 331–342
29. Purohit, A., Tynan, S. H., Vallee, R., and Doxsey, S. J. (1999) *J. Cell Biol.* **147,** 481–492
30. Tynan, S. H., Purohit, A., Doxsey, S. J., and Vallee, R. B. (2000) *J. Biol. Chem.* **275,** 32763–32768
31. Orr, J. W., and Newton, A. C. (1994) *J. Biol. Chem.* **269,** 27715–27718
32. Keranen, L. M., Dutil, E. M., and Newton, A. C. (1995) *Curr. Biol.* **5,** 1394–1403
33. Murray, N. R., Baumgardner, G. P., Burns, D. J., and Fields, A. P. (1993) *J. Biol. Chem.* **268,** 15847–15853
34. Stearns, T., and Kirschner, M. (1994) *Cell* **76,** 623–637
35. Yu, W., Murray, N. R., Weems, C., Chen, L., Guo, H., Ethridge, R., Ceci, J. D., Evers, B. M., Thompson, E. A., and Fields, A. P. (2003) *J. Biol. Chem.* **278,** 11167–11174
36. Pihan, G. A., Purohit, A., Wallace, J., Knecht, H., Woda, B., Quesenberry, P., and Doxsey, S. J. (1998) *Cancer Res.* **58,** 3974–3985
37. Pihan, G. A., Wallace, J., Zhou, Y., and Doxsey, S. J. (2003) *Cancer Res.* **63,** 1398–1404
38. Leitges, M., Schmedt, C., Guinamard, R., Davoust, J., Schaal, S., Stabel, S., and Tarakhovsky, A. (1996) *Science* **273,** 788–791
39. Meraldi, P., Honda, R., and Nigg, E. A. (2002) *EMBO J.* **21,** 483–492
40. Seong, Y. S., Kamijo, K., Lee, J. S., Fernandez, E., Kuriyama, R., Miki, T., and Lee, K. S. (2002) *J. Biol. Chem.* **277,** 32282–32293
41. Gokmen-Polar, Y., Murray, N. R., Velasco, M. A., Gatalica, Z., and Fields, A. P. (2001) *Cancer Res.* **61,** 1375–1381
42. Nakhost, A., Kabir, N., Forscher, P., and Sossin, W. S. (2002) *J. Biol. Chem.* **277,** 40633–40639
43. Hosotani, T., Koyama, H., Uchino, M., Miyakawa, T., and Tsuchiya, E. (2001) *Genes Cells* **6,** 775–788
44. Cox, D. N., Seyfried, S. A., Jan, L. Y., and Jan, Y. N. (2001) *Proc. Natl. Acad. Sci. U. S. A.* **98,** 14475–14480
45. Radoja, S., Saio, M., Schaer, D., Koneru, M., Vukmanovic, S., and Frey, A. B. (2001) *J. Immunol.* **167,** 5042–5051
46. Vanzela, A. P., and Said, S. (2002) *Microbiol. Res.* **157,** 239–247
47. Parissenti, A. M., Kim, S. A., Colantonio, C. M., Snihura, A. L., and Schimmer, B. P. (1996) *J. Cell. Physiol.* **166,** 609–617
48. Yamaguchi, K., Ogita, K., Nakamura, S., and Nishizuka, Y. (1995) *Biochem. Biophys. Res. Commun.* **210,** 639–647
49. Zong, Z. P., Fujikawa-Yamamoto, K., Teraoka, K., Yamagishi, H., Tanino, M., and Odashima, S. (1994) *Biochem. Biophys. Res. Commun.* **205,** 746–750
50. Bement, W. M., and Capco, D. G. (1991) *Cell Motil. Cytoskeleton* **20,** 145–157
51. Bement, W. M., and Capco, D. G. (1989) *J. Cell Biol.* **108,** 885–892
52. Khalfan, W., Ivanovska, I., and Rose, M. D. (2000) *Genetics* **155,** 1543–1559
53. Diviani, D., Langeberg, L. K., Doxsey, S. J., and Scott, J. D. (2000) *Curr. Biol.* **10,** 417–420
54. Diviani, D., and Scott, J. D. (2001) *J. Cell Sci.* **114,** 1431–1437